Published in final edited form as:
J Tissue Eng Regen Med. 2009 December ; 3(8): 590–600. doi:10.1002/term.200.

Evidence of Innervation following Extracellular Matrix Scaffold Mediated Remodeling of Muscular Tissues

Vineet Agrawal[a,b,d], **Bryan N. Brown**[a,b], **Allison J. Beattie**[a,c], **Thomas W. Gilbert**[a,b,c], and **Stephen F. Badylak**[a,b,c]

[a] McGowan Institute for Regenerative Medicine, University of Pittsburgh, Pittsburgh, PA

[b] Department of Bioengineering, University of Pittsburgh, Pittsburgh, PA

[c] Department of Surgery, University of Pittsburgh, Pittsburgh, PA

[d] Medical Scientist Training Program, University of Pittsburgh, Pittsburgh, PA

Abstract

Naturally occurring porcine derived extracellular matrix (ECM) has successfully been used as a biologic scaffold material for site-specific reconstruction of a wide variety of tissues. The site-specific remodeling process includes rapid degradation of the scaffold with concomitant recruitment of mononuclear cells, endothelial cells, and bone marrow derived cells, and can lead to formation of functional skeletal and smooth muscle tissue. However, the temporal and spatial patterns of innervation of the remodeling scaffold material in muscular tissues are not well understood. A retrospective study was conducted to investigate the presence of nervous tissue in a rat model of abdominal wall reconstruction and a canine model of esophageal reconstruction in which ECM scaffolds were used as inductive scaffolds. Evidence of mature nerve, immature nerve, and Schwann cells was found within the remodeled ECM at 28 days in the rat body wall model, and at 91 days post surgery in a canine model of esophageal repair. Additionally, a microscopic and morphologic study that investigated the response of primary cultured neurons seeded upon an ECM scaffold showed that neuronal survival and outgrowth was supported by the ECM substrate. Finally, matricryptic peptides resulting from rapid degradation of the ECM scaffold induced migration of terminal Schwann cells in a concentration dependent fashion in vitro. The findings of this study suggest that the reconstruction of tissues in which innervation is an important functional component is possible with use of biologic scaffolds composed of extracellular matrix.

Introduction

Innervation is implicit to the success of tissue engineering and regenerative medicine strategies with an end goal of functional tissue restoration. Numerous studies have investigated in vitro the ability of naturally derived (Hadlock et al., 2001; Smith et al., 2004; Phillips et al., 2005; Donzelli et al., 2006; Su et al., 2007; Chunzheng et al., 2008) and artificially synthesized (Johansson et al., 2006; Recknor et al., 2006; Gomez et al., 2007; Schnell et al., 2007; Sorensen et al., 2007) biomaterials to support neuronal outgrowth and differentiation. However, relatively few studies have investigated the process of innervation following in vivo placement of such biomaterials or tissue engineered constructs (Pope et al., 1997; Patrick et al., 2001; Caione et al., 2006; Caissie et al., 2006; Lopes et al., 2006; Ueno et al., 2007).

Corresponding author: Stephen F. Badylak, McGowan Institute for Regenerative Medicine, University of Pittsburgh, 100 Technology Drive, Suite 200, Pittsburgh, PA 15219, P: (412) 235-5144, F: (412) 235-5110, badylaks@upmc.edu.

Biologic scaffold materials composed of extracellular matrix (ECM) have been used in preclinical animal studies and human clinical applications to facilitate constructive remodeling of a variety of muscular tissues including esophagus (Badylak et al., 2000; Badylak et al., 2005; Lopes et al., 2006), myocardium (Kochupura et al., 2005; Robinson et al., 2005; Badylak et al., 2006; Ota et al., 2007), blood vessels (Badylak et al., 1989; Lantz et al., 1990; Lantz et al., 1992), urinary bladder (Kropp et al., 1995; Kropp et al., 1996; Pope et al., 1997; Record et al., 2001), and skeletal muscle (Prevel et al., 1995; Clarke et al., 1996; Badylak et al., 2001; Badylak et al., 2002). Following implantation of the ECM scaffold, these studies have shown that the host response is characterized by rapid degradation of the scaffold with concomitant replacement by organized, site-appropriate, functional host tissue (Allman et al., 2001; Record et al., 2001; Allman et al., 2002; Gilbert et al., 2007).

The mechanisms responsible for the remodeling response following placement of an ECM scaffold are not fully understood, but are thought to include bioactive matricryptic peptides generated following rapid scaffold degradation (Record et al., 2001; Li et al., 2004; Brennan et al., 2006; Gilbert et al., 2007; Gilbert et al., 2007), recruitment of both differentiated and multi-potential cells to the site of remodeling (Badylak et al., 2002; Valentin et al., 2006; Zantop et al., 2006), angiogenesis (Badylak et al., 2000; Li et al., 2004), and deposition of site-appropriate tissue in response to appropriate mechanical cues (Gilbert et al., 2006; Gilbert et al., 2007). However, the contribution of nervous tissue to the remodeling process has not been investigated.

Recent studies compared the in vivo remodeling of commercially available ECM scaffold devices in a rat model of abdominal wall repair (Valentin et al., 2006; Brown et al., In press). Islands of morphologically normal skeletal muscle replaced portions of acellular, ECM scaffolds that have not been chemically cross-linked within the first 28 days of the remodeling process. However, it was not reported whether these islands of muscle were innervated and functional. An earlier study of ECM-mediated esophageal reconstruction showed peristalsis in positive contrast esophagrams and spontaneous contraction immediately after euthanasia (Badylak et al., 2005). ECM scaffold remodeling in the urinary bladder (Pope et al., 1997; Caione et al., 2006) and stomach (Ueno et al., 2007) has shown innervation of new muscle tissue. It is logical that morphologically normal appearing skeletal or smooth muscle formed during remodeling of an ECM scaffold would be accompanied by a motor nerve supply.

The objective of the present study was to determine the temporal and spatial patterns of innervation during the process of ECM scaffold remodeling through a retrospective analysis of animal models of esophageal and body wall reconstruction (Badylak et al., 2005; Brown et al., In press). Additionally, in vitro studies were performed to determine the ability of an ECM scaffold to support attachment and survival of a neuronal cell population, and the ability of ECM matricryptic peptides to recruit cells known to support neuronal regeneration.

Methods

Overview

A retrospective analysis was conducted to determine the temporal appearance and spatial distribution of innervation at the site of ECM remodeling in two separate studies of rat abdominal wall reconstruction (Brown et al., In press) and canine esophageal repair (Badylak et al., 2005) (Table 1). The biologic scaffold material used in both studies consisted of ECM derived from the porcine urinary bladder (UBM). Immunohistochemical methods were used to identify the presence of mature nerve (neurofilament), growing nerves

(GAP-43) (Goslin et al., 1990), and the presence of Schwann cells (GFAP – glial fibrillary acidic protein) (Triolo et al., 2006) in the tissues of interest. GFAP was chosen as the marker for Schwann cells because previous studies have demonstrated that Schwann cells retain expression of GFAP following dedifferentiation while losing the expression of other mature markers such as S-100 (Jessen and Mirsky, 1991; Garavito et al., 2000; Triolo et al., 2006). In a separate prospective study, primary spinal cord neurons were isolated from embryonic rat spinal cords and cultured upon UBM, and examined for the expression of neuron and glial specific markers (β-tubulin-III and GFAP) by immunofluorescent labeling techniques. Finally, the migration of Schwann cells in response to matricryptic peptides from UBM was investigated in a Boyden chamber assay.

All methods were approved by the Institutional Animal Care and Use Committee at the University of Pittsburgh and performed in compliance with NIH Guidelines for the Care and Use of Laboratory Animals.

Preparation of Urinary Bladder Matrix

The urinary bladder matrix was prepared using previously described methods (Freytes et al., 2004; Robinson et al., 2005). Briefly, porcine urinary bladders were harvested from market weight pigs (approximately 110–130 kg) immediately after sacrifice. Residual external connective tissues, including adipose tissue, were trimmed and all residual urine was removed by repeated washes with tap water. The urothelial layer was removed by soaking of the material in 1 N saline. The tunica serosa, tunica muscularis externa, tunica submucosa, and most of the muscularis mucosa were mechanically delaminated from the bladder tissue. The remaining basement membrane of the tunica epithelialis mucosa and the subjacent tunica propria were collectively termed UBM. The UBM was decellularized and disinfected by immersion in 0.1% (v/v) peracetic acid (PAA) (σ), 4% (v/v) ethanol, and 96% (v/v) deionized water for 2 h. The material was then washed twice for 15 min with phosphate buffered saline (PBS) (pH = 7.4) and twice for 15 min with deionized water.

Rat Abdominal Wall Model

Preparation of 4-layer body wall ECM device—Multilaminate (4-layer) sheets were constructed as previously described (Freytes et al., 2004). In brief, four hydrated sheets of UBM were stacked on top of one another, each at a 90° orientation to the adjacent layers. The constructs were then placed into plastic pouches and attached to a vacuum pump (Leybold, Export, PA, Model D4B) with a condensate trap inline. The constructs were subjected to a vacuum of 710 to 740 mm Hg for 10 to 12 h to remove the water and form a tightly coupled multilaminate construct. The devices were terminally sterilized with ethylene oxide.

Surgical Procedure—The surgical procedure of the partial thickness rat abdominal wall reconstruction has been previous described (Badylak et al., 2002; Brown et al., In press). A ventral midline incision was made and the adjacent subcutis dissected to expose the ventral lateral abdominal wall. A 1 cm × 1 cm partial thickness defect was then created in the exposed musculature, leaving the underlying peritoneum, transversalis fascia, transversus abdominis and the overlying skin intact. The muscular defects were reconstructed with a UBM test article. The test article was sutured to the adjacent abdominal wall with 4-0 Prolene non-absorbable suture at each corner to secure test article and to allow for identification of the device boundaries at the time of euthanasia and explantation. The skin was closed using absorbable 4-0 Vicryl suture. The animals were recovered from anesthesia on a heating pad and allowed normal activity and diet for the remainder of the study period. Animals were euthanized at time points of 3, 7, 14, and 28 days and the defect site was excised with a small portion of the surrounding native tissue.

Canine Esophageal Resection Study

Device preparation—Multilayer tubes were created by wrapping hydrated sheets of UBM around a 30 mm perforated tube/mandrel that was covered with umbilical tape for a total of four complete revolutions (i.e., a four layer tube)(Kochupura et al., 2005). The constructs were then placed into plastic pouches and attached to a vacuum pump (Leybold, Export, PA, Model D4B) with a condensate trap inline. The constructs were subjected to a vacuum of 710 to 740 mm Hg for 10 to 12 h to remove the water and form a tightly coupled multilaminate construct. After removal of each device from the mandrel, they were terminally sterilized with ethylene oxide.

Surgical Procedure—Surgical procedures were completed as reported (Badylak et al., 2005). Briefly, adult female mongrel dogs weighing between 17 and 24 kg were divided into four groups and subjected to surgical resection of 5 cm of the full circumference of the esophageal endomucosa (epithelium, basement membrane, lamina propria, muscularis mucosa, and tunica submucosa) with removal of varying amounts of the muscularis externa. Four surgical groups were investigated in the canine study, as listed in Table 1. In group 1, the full thickness of the 5 cm esophageal segment was removed and the defect was repaired with a tubular UBM scaffold. In group 2, all layers of the esophagus except for the muscularis externa were removed, and the defect was untreated to serve as a control. In group 3, 70% of the circumference of the 5 cm segment of esophagus was subjected to full thickness resection and the defects were repaired with a tubular UBM scaffold. Finally, group 4 was the same as group 2, with the exception that the resected endomucosal tissue was replaced with a tubular UBM scaffold. In groups 3 and 4, the UBM was sutured to the native endomucosa using 5-0 prolene sutures and the muscle and subcutaneous tissues were closed with 4-0 Vicryl sutures. Following surgery the animals were recovered from anesthesia and allowed normal ambulation. The animals were given soft food from a raised bowl for two weeks or until they could tolerate normal diet. At the time of sacrifice, the defect site was excised with a small portion of the adjacent native tissue. For the present study, sections the remodeled scaffold from 3 animals from group 3 that had been sacrificed at 91, 101, and 104 days after surgery were examined for markers of nervous tissue. Sections from the animal in group 2 that showed a scar tissue response with stricture served as a negative control. Sections from an animal in group 4 that had normal intact muscle served as a positive control for immunohistochemical studies.

Immunohistochemistry of Animal Sections

Paraffin embedded specimens from both studies were cut into 6 μm thick sections and mounted on to glass slides. The specimens were deparaffinized by treatment with xylene and exposure to a graded series of ethanol (100-70%). Following deparaffinization, the slides were placed in citrate antigen retrieval buffer (10mM citric acid monohydrate, pH 6.0, C1285, Spectrum, New Brunswick, NJ) at 95–100°C for 20 minutes. The buffer was allowed to cool to room temperature on ice and the slides were washed twice in Tris buffered saline/Tween 20 (Trizma Base, T6066, Sigma; Tween 20, P7949, Sigma, St. Louis, MO) solution (pH 7.4) and twice in PBS. The sections were then incubated in 2% normal horse serum (S-2000, Vector, Burlingham, CA) for 1 hour at room temperature in a humidified chamber to inhibit non-specific binding of the primary antibody. Following incubation in blocking serum, the sections were incubated in primary antibody in a humidified chamber at 4°C overnight. Each tissue specimen was exposed to antibodies to the light chain of neurofilament (Anti-neurofilament, M0762, DakoUSA, Carpinteria, CA), to a marker that localizes to the growth cones of regenerating neurons (Anti-GAP43, NB600, Novus Biologicals, Littleton, CO), or to a marker that is known to localize to Schwann cells in the peripheral nervous system following injury (Anti-GFAP, M0761, DakoUSA). Following overnight incubation, the slides were washed three times in PBS.

Sections were then incubated in a solution of 3% H_2O_2 in methanol for 30 minutes at room temperature to quench any endogenous peroxidase activity. Following H_2O_2 treatment, the slides were washed three times in PBS and incubated in secondary antibody for 30 min in a humidified chamber at room temperature prior to three more washes in PBS. The sections were then incubated in Vectastain ABC (Elite ABC kit, PK6200, Vector Labs, Burlingame, CA) reagent for 30 min in a humidified 37°C chamber, rinsed 3 times in PBS, and incubated in 4% diaminobenzadine substrate solution (SK4100, Vector Labs) at room temperature until the slides showed the desired staining affinity. Finally, the slides were rinsed in water to stop the development of the diaminobenzadine substrate and counterstained using Harris' hematoxylin stain (Thermo Electron Corp.-Shandon, Pittsburgh, PA). The slides were then dehydrated using the reverse of the deparaffinization treatment described above and then coverslipped. Each PBS rinse in the protocol was for 3 minutes at room temperature, with occasional agitation.

Anti-neurofilament antibody was used at a concentration of 1:100. Anti-GAP43 was used at a concentration of 1:250. Anti-GFAP antibody was used at a concentration of 1:500. Corresponding secondary antibodies were used at a concentration of 1:100 for biotinylated anti-mouse IgG (Vector Labs, BA-2000) and 1:200 for biotinylated anti-rabbit IgG (PK-4001, Vector Labs). All antibodies were diluted in filtered PBS (pH 7.4). Native canine esophagus and rat abdominal wall were used as positive control tissue samples for staining.

Culture of Neurons on UBM

Isolation of Embryonic Spinal Cord Neurons—Spinal cord neurons were isolated from embryonic day 14 Sprague Dawley rat pups. Spinal cords were collected in cold Hank's buffered salt solution without Ca^{2+} and Mg^{2+} (14170-112, Gibco, Carlsbad, CA), minced into pieces approximately 0.5mm^2 in size, and enzymatically dissociated in 2 ml of 0.25% trypsin solution containing 0.05% collagenase L1 (MP Biomedicals, Solon, OH) at 37 °C for 20 min. Cell digestion was inhibited by adding 2ml SBTI-DNAse solution (0.52mg/ml soybean trypsin inhibitor, T-9003; 3.0 mg/ml BSA, A-2153; 0.04mg/ml bovine pancreas DNAse, D-4263; Sigma). The cell suspension was gently triturated with a Pasteur pipette, and centrifuged at 800g for 5 min. The resulting pellet was then resuspended in plating medium and gently triturated. Plating medium consisted of 20% horse serum (16050-130, Gibco), 2 mM L-glutamine (25030-081, Gibco), 5 ml HBSS without Ca^{2+} and Mg^{2+} (14170-112, Gibco), and 9.8 ml Dulbecco's Modified Eagles Medium (DMEM) (D5648, Sigma). All non-dispersed tissue was allowed to settle before being discarded.

Cell Seeding—Single sheets of UBM were cut with a 1.5 cm diameter circular punch to create discs for use in cell culture experiments. Using sterile stainless steel rings to anchor the UBM discs, spinal cord neurons were seeded on the abluminal surface of the discs in plating medium at a plating density of 3×10^5 cells/cm^2 and allowed to adhere for 4 hours in culture conditions of 5% CO_2 and 37 °C in humidified environment. After four hours, medium was exchanged with 1 ml of serum-free culture medium containing Neurobasal-A (NBA, 10888-022, Gibco), 1x B27 supplement and 1mM glutamax (35050-061, Gibco). Cells were maintained in a humidified 5% CO_2 atmosphere at 37°C, with 50% of the culture medium changed every 4 days. Cells were seeded at the same concentration on poly-L-lysine coated cover slips (12.5μg/ml in H_2O, P1274, Sigma, St. Louis, MO) as a control.

Immunofluorescent Labeling—Cells seeded on control cover slips were maintained in culture for 5 days. They were then washed 3 times with PBS warmed to 37 °C, fixed with 4% formaldehyde at 37 °C for 15 min, and incubated in permeablization buffer (0.5% Triton X) for 15 min at room temperature. All antibodies were diluted to working concentration in a modified PBS solution (0.3 M NaCl PBS, 0.3% Triton X). All primary antibodies were

diluted to a working dilution of 1:100 and incubated overnight at 4 °C. All secondary antibodies, also at a working dilution of 1:100, were incubated for 1 hour at 37 °C. After each stage of antibody incubation, samples were gently washed 3 times for 5 min in PBS. Samples were examined using antibodies against β-tubulin III (Sigma) and GFAP (DakoUSA) and secondary antibodies, FITC conjugated goat anti-mouse IgG_{2b} and TRITC conjugated goat anti-rabbit (Cambridge Biosciences, Cambridge, UK), respectively. All samples were mounted in Vectashield mounting medium containing DAPI (Vector Laboratories Burlingame, CA, USA).

The UBM cell-seeded discs were harvested after 5 days and fixed with 10% neutral buffered formalin for 24 hours. Sections of the discs were trimmed, embedded in paraffin and then cut, in cross sections, into 5μm thick sections. All sections were first deparaffinized before being immersed in permeablization buffer (0.5% Triton X) for 15 min at room temperature. Sections were triple-stained as described above with and without the primary antibodies.

Preparation of Samples for SEM Analysis—All samples examined by SEM were fixed for 2 hours with 2.5% gluteraldehyde. After three 15 min washes in PBS, samples were dehydrated through a graded series of ethanol washes, followed by chemical drying with 100% hexamethyldisilazane (HMDS) overnight. Samples were sputter coated with a 4 nm thick layer of gold palladium (Cressington 108 sputter coater, Cressington, UK) and then examined using a JEM 6335F field emission gun SEM (JEOL, Peabody, MA) with an excitation voltage of 4kV.

Migration and Survival of Schwann cells in Response to ECM degradation

Formation of Peptide Fragments of UBM—The preparation of UBM matricryptic peptides has previously been described (Reing et al., 2008). UBM was digested with pepsin by mixing 1 g of lyophilized, powdered UBM with 100 mg pepsin (Sigma-Aldrich, St. Louis, MO) in 100 ml of 0.01M HCl. The pepsin was allowed to digest the UBM for 48 hours under constant stir at 4 °C. The pepsin was inactivated by bringing the mixture to a pH of 7.4 using PBS, and the resulting peptide fragments were used in migration and survival assays at concentrations of 50 μg/ml, 100 μg/ml, and 200 μg/ml of dry weight protein.

Cell Migration Assay—Schwann cells (RT4-D6P2T cell line) were obtained from the ATCC and cultured in medium containing DMEM, 10% FBS, 100 U/ml penicillin, and 100 μg/ml streptomycin. Passages 2–4 were utilized for the present study. Cells at 70–80% confluence were starved in serum-free DMEM for 16 hours. After starvation, cells were trypsinized with 0.25% trypsin and 0.53 mM EDTA for 2 minutes, and resuspended in culture medium. Cells were centrifuged at 1200 rpm (Sorvall Legend RT, Heraeus 6445 rotor) for 5 min, and the pellet was re-suspended in serum-free DMEM and incubated in a humidified environment at 37 °C in 5% CO_2 for 1 hour. Polycarbonate PFB filters (Neuro Probe, Gaithersburg, MD) with pore size 8 μm were coated on both sides with 0.05 mg/ml Collagen Type I (BD Biosciences, San Jose, CA). Peptide fragments of UBM were placed in the bottom chamber of Neuro Probe 48-well migration chambers (Neuro Probe, Gaithersburg, MD), and the filter was then placed over the bottom chamber. The upper chamber was then assembled onto the lower chamber and sealed. Approximately 30,000 cells were placed in to each well of the top chamber, and the entire system was placed in a humidified environment at 37 °C in 5% CO_2 for 3 hours. After three hours, cells facing the upper chamber on the filter were scraped off, and cells facing the bottom filter were fixed in methanol and stained with DiffQuick (Dade AG Liederbach, Germany). Each concentration of peptide fragments was run in quadruplicate, and the results of each condition were compared to the results of a buffer control that contained all components at the same concentration except for the peptide fragments. The total number of migrated cells in each

well was then counted, and a mean number of migrated cells were calculated from the quadruplicates sample. The experiment was repeated three times, and the values for the chemotactic activity obtained for the peptide fragments and control were compared via Student's T-test (2-tailed, unequal variance).

Survival Assay—Schwann cells at 70–80% confluence were starved in serum-free DMEM for 16 hours. After starvation, cells were trypsinized with 0.25% trypsin and 0.53 mM EDTA for 2 minutes, and resuspended in culture medium. Cells were centrifuged at 1200 rpm for 5 min, re-suspended in serum-free DMEM, and incubated in a humidified environment at 37 °C in 5% CO_2 for 1 hour. In each well of a 96 well plate, 8,000 cells were plated in serum-free DMEM. Varying concentrations of peptide fragments or corresponding buffer controls were added to wells. Culture medium was used in positive control wells. After 48 hours, supernatant was removed and samples were extensively washed in PBS, lysed, and cell number was assayed using the Cambrex ViaLight™ Plus Cell Proliferation Kit (Cambrex Corp.) and M2 SpectraMax plate reader. Each condition was tested in triplicate, and the assay was repeated three times. Differences were assessed via Student's T-test (2-tailed, unequal variance).

Results

Rat Abdominal Wall Model

Following abdominal wall repair in the rodent model, the UBM scaffold showed progressive remodeling with time. Histologic examination showed a mixture of skeletal muscle cells and organized collagenous connective tissue at the site of UBM placement at day 28. No positive staining for neurons or Schwann cells was present at days 3, 7, and 14. At day 28, positive staining for neurons was observed in the remodeled UBM-ECM scaffold adjacent to the leading edge of growth of the adjacent native external oblique muscle. Nerves were localized to regions of neo-muscular growth. Positive staining for GAP-43 confirmed that these nerves were actively growing (Skene and Willard, 1981; Hoffman, 1989; Goslin et al., 1990). Positive stain for Schwann cells colocalized with positive stain for nerves within the pockets of neo-muscular growth (Figure 2). The specificity of neurofilament, GFAP, and GAP-43 stains was confirmed via staining of nerve in native rat abdominal wall muscle.

Canine Esophageal Model

Histologic examination showed the presence of a well defined muscularis externa, tunica submucosa, tunica mucosa with complete endothelium. The remodeled tissue differed from normal esophagus in that the remodeled esophagus lacked rugal folds, mature rete pegs in the epithelium, and glandular structures in the submucosa (Badylak et al., 2005). Muscular tissue subjacent to the submucosa was examined for the presence of neural tissue. Schwann cells and regenerating neurons were observed adjacent to mature skeletal muscle cells in all three specimens at 91, 101, and 104 days post-surgery (Figure 3). In a region of neo-muscular growth, positive staining for Schwann cells and GAP-43 was present in the absence of positive staining for neurofilament (Figure 4). Positive staining was confirmed in the myenteric plexus of samples from Group 4 where the muscularis externa was left intact (Figure 5). In samples from Group 2 (scar tissue with stricture), there was a lack of organized muscularis mucosa and externa and incomplete epithelialization. No evidence of nerve was present in these samples.

Neuronal Survival and Axonal Outgrowth on UBM

Approximately 90% of cells isolated from the spinal cord tissue of embryonic Sprague Daly rat pups and grown on control cover slips were positively labeled for the neuron specific cytoskeletal marker β-tubulin-III and were therefore classified as neurons (Figure 6a). To

confirm that the cells and corresponding cell processes attached to the abluminal scaffold surface were neurons, sections were labeled for β-tubulin-III and glial marker GFAP. Cells seeded on the scaffold surface stained positive for both cytoskeletal markers (β-tubulin-III and GFAP) (Figures 6b, 6c). SEM analysis showed that seeded cells displayed long cellular processes that spanned the inter-fibril spaces of the abluminal surface structure (Figures 7a, 7b). At high magnification, it was evident that cellular processes were interacting with the surface structure (Figure 7c).

Peptide Fragments following Degradation of UBM scaffold Recruit Schwann cells

A concentration dependent increase in migration of Schwann cells towards UBM peptide fragments was noted, and migration at all concentrations was increased compared to buffer controls at each concentration and positive control fibronectin (Figure 8a). The only concentration for which an increase in cell survival compared to the negative control was noted was at a concentration of 50 μg/ml (Figure 8b).

Discussion

This retrospective study showed the presence of nerve tissue within sites of ECM scaffold remodeling, first observed at 28 days in the rat model and at 91 days in the canine model. While sites of positive staining did not morphologically match the appearance of normal nerve fibers in muscle, these results are in accordance with the findings that ECM reconstructed esophagus showed positive contrast esophagrams and spontaneous contraction during dissection at necropsy (Badylak et al., 2000). Because modeling as a result of implantation of a biologic scaffold did not result in complete reformation of structures normally found in histologic sections of the esophagus and abdominal wall, it is possible that nerve fibers also repopulated the site of remodeling and did not resemble what is seen in normal sections. The initial appearance of neuronal axons in both models was spatially and temporally associated with the presence of new muscle tissue. In addition, the present study demonstrated that the surface topology of the ECM scaffold itself supports in vitro neuronal outgrowth and survival. Finally, the present study shows that degradation of the ECM scaffold can produce peptide fragments that recruit Schwann cells. Overall, the findings of the present study support the hypothesis that functional remodeling of ECM scaffolds is associated with the presence of mature and regenerating nerve.

The present findings are consistent with previous studies that have shown innervation of the urinary bladder and esophagus after repair with an ECM scaffold composed of porcine small intestinal submucosa (SIS-ECM) (Pope et al., 1997; Caione et al., 2006; Lopes et al., 2006). Although it is not known whether ECM scaffolds derived from other tissue and organs (i.e., liver, skin, and pericardium) can also support innervation during the process of *in vivo* remodeling, it is likely that innervation is a requisite component of any functional tissue remodeling that occurs, regardless of the tissue source of the ECM scaffold used. ECM scaffolds may have an advantage over synthetic scaffolds in this regard since they are secreted by the resident cells of each tissue, and the matrix is likely optimized to support the maintenance of cell phenotypes native to that tissue (Sellaro et al., 2007).

A number of studies have shown that soluble factors released from ECM and the degradation products themselves are capable of recruiting both differentiated cells and progenitor cells to the site of remodeling (Li et al., 2004; Reing et al., 2008). The present study demonstrated that peptides resulting from rapid degradation of ECM scaffolds are chemoattractant for Schwann. Following injury and denervation, the terminal Schwanns cell covering the neuromuscular junction are induced to proliferate and guide the neuronal axon back to the muscle (Sanes, 1983; Sanes, 1989; Grinnell, 1995; La Fleur et al., 1996; Son et al., 1996; Auld and Robitaille, 2003; Reddy et al., 2003). Thus, the directed migration of the

RT4-D6P2T cell line, a model for terminal Schwann cells (Bansal and Pfeiffer, 1987; Ponomareva et al., 2006), suggests that terminal Schwann cells may be at least partially responsible for the ECM mediated neurite outgrowth in to the site of remodeling.

The temporal and spatial association between nerve and muscle in the current and previous studies (Pope et al., 1997) suggests that either these cell types or their precursors all respond to the same stimulus, or more likely, participate in paracrine interaction or direct cell-to-cell communication that supports their simultaneous growth and development. Previous developmental studies show that nerves can create a myotrophic environment to promote the recruitment of muscle (Brockes, 1984; Dietz, 1989; Ashby et al., 1993; Suzuki et al., 2005). The reciprocal neurotrophic effect of muscle formation is well known in both developmental and regenerative models (McCaig, 1986; Grinnell, 1995; Carlson, 2005; Kingham and Terenghi, 2006). The dual neurotrophic and angiogenic effects of blood vessels and nerves, respectively, have also been extensively studied (Carmeliet, 2003), and nerve may in fact guide the growth of blood vessels in normal development *in vivo* (Mukouyama et al., 2002).

The interactions between these cells types are not well understood in the context of biologic scaffolds and regenerative medicine. The ability of ECM scaffolds to recruit and support endothelial cells (Stupack and Cheresh, 2002; Li et al., 2004; Sellaro et al., 2007) and muscle cells (Prevel et al., 1995; Clarke et al., 1996; Kropp et al., 1996; Pope et al., 1997; Badylak et al., 2000; Badylak et al., 2002; Badylak et al., 2005; Caione et al., 2006; Ueno et al., 2007) is well known. It is not clear whether neuronal axons first promote the recruitment of endothelial cells and muscle cells, or whether endothelial cells and muscle cells promote the directed outgrowth of neurons at the site of injury.

While the present study has demonstrated that nerve fibers and associated Schwann cells repopulate the remodeled tissue as a result of implantation of a biologic scaffold composed of ECM, it is not clear whether the nervous tissue is functional. Although the present study did not assess functionality, it is plausible that a number of the nerve fibers observed in the present study could eventually reform functional connections. Because tissue remodeling was likely still active within the tissues investigated (Gilbert et al., 2007), the process of functional innervation may not have reached equilibrium at the time of sacrifice. Thus, it would be expected that any functional innervation of muscle was not complete at the time.

Additionally, the present study cannot distinguish between various subsets of neurons such as motor, general sensory, and nociceptive sensory neurons in the site of remodeling. However, retrospective immunhistochemical analysis to distinguish between various subsets of neurons is not reliable in a regenerative setting because expression of subset-specific markers and genes is altered following injury to peripheral nerves (Navarro et al., 2007). Future studies that prospectively assess functionality and phenotype of nerves in vivo and ex vivo will be required to adequately understand the nature of the regenerated neuronal axons.

In summary, the collective findings of this retrospective study and previous studies (Pope et al., 1997; Caione et al., 2006; Lopes et al., 2006; Ueno et al., 2007) shows that mature and regenerating nerve tissue is present in the site of remodeling following placement of an ECM scaffold. Further investigation of the mechanisms underlying the process of innervation during in vivo ECM scaffold remodeling is needed. By understanding the mechanisms that promote innervation, it may be possible to control the spatio-temporal patterns of innervation and ultimately promote faster remodeling of functional, site-appropriate tissue.

Conclusions

The findings of this study demonstrate the temporal and spatial association of innervation during the in vivo remodeling of the ECM scaffold used for reconstruction of two muscular tissues: the esophagus and muscular body wall. Further investigation in well designed prospective studies is warranted and needed.

Acknowledgments

The authors would like to thank Jennifer DeBarr for her assistance in preparation of the histologic sections. The authors would also like to thank the Center for Biological Imaging Core Facility at the University of Pittsburgh for the use of their equipment for imaging. This work was supported by NIH 5R01 AR054940O3.

References

Allman AJ, McPherson TB, Badylak SF, Merrill LC, Kallakury B, Sheehan C, Raeder RH, Metzger DW. Xenogeneic extracellular matrix grafts elicit a TH2-restricted immune response. Transplantation. 2001; 71(11):1631–40. [PubMed: 11435976]

Allman AJ, McPherson TB, Merrill LC, Badylak SF, Metzger DW. The Th2-restricted immune response to xenogeneic small intestinal submucosa does not influence systemic protective immunity to viral and bacterial pathogens. Tissue Eng. 2002; 8(1):53–62. [PubMed: 11886654]

Ashby PR, Wilson SJ, Harris AJ. Formation of primary and secondary myotubes in aneural muscles in the mouse mutant peroneal muscular atrophy. Dev Biol. 1993; 156(2):519–28. [PubMed: 8462748]

Auld DS, Robitaille R. Perisynaptic Schwann cells at the neuromuscular junction: nerve- and activity-dependent contributions to synaptic efficacy, plasticity, and reinnervation. Neuroscientist. 2003; 9(2):144–57. [PubMed: 12708618]

Badylak S, Kokini K, Tullius B, Simmons-Byrd A, Morff R. Morphologic study of small intestinal submucosa as a body wall repair device. J Surg Res. 2002; 103(2):190–202. [PubMed: 11922734]

Badylak S, Kokini K, Tullius B, Whitson B. Strength over time of a resorbable bioscaffold for body wall repair in a dog model. J Surg Res. 2001; 99(2):282–7. [PubMed: 11469898]

Badylak S, Meurling S, Chen M, Spievack A, Simmons-Byrd A. Resorbable bioscaffold for esophageal repair in a dog model. J Pediatr Surg. 2000; 35(7):1097–103. [PubMed: 10917304]

Badylak SF, Kochupura PV, Cohen IS, Doronin SV, Saltman AE, Gilbert TW, Kelly DJ, Ignotz RA, Gaudette GR. The use of extracellular matrix as an inductive scaffold for the partial replacement of functional myocardium. Cell Transplant. 2006; 15 (Suppl 1):S29–40. [PubMed: 16826793]

Badylak SF, Lantz GC, Coffey A, Geddes LA. Small intestinal submucosa as a large diameter vascular graft in the dog. J Surg Res. 1989; 47(1):74–80. [PubMed: 2739401]

Badylak SF, Vorp DA, Spievack AR, Simmons-Byrd A, Hanke J, Freytes DO, Thapa A, Gilbert TW, Nieponice A. Esophageal reconstruction with ECM and muscle tissue in a dog model. J Surg Res. 2005; 128(1):87–97. [PubMed: 15922361]

Bansal R, Pfeiffer SE. Regulated galactolipid synthesis and cell surface expression in Schwann cell line D6P2T. J Neurochem. 1987; 49(6):1902–11. [PubMed: 2824698]

Brennan EP, Reing J, Chew D, Myers-Irvin JM, Young EJ, Badylak SF. Antibacterial activity within degradation products of biological scaffolds composed of extracellular matrix. Tissue Eng. 2006; 12(10):2949–55. [PubMed: 17518662]

Brockes JP. Mitogenic growth factors and nerve dependence of limb regeneration. Science. 1984; 225(4668):1280–7. [PubMed: 6474177]

Brown BN, Valentin JE, Stewart-Akers AM, McCabe GP, Badylak SF. Biologic Scaffold Remodeling and Macrophage Polarization in a Rat Body Wall Model. Biomaterials. In press.

Caione P, Capozza N, Zavaglia D, Palombaro G, Boldrini R. In vivo bladder regeneration using small intestinal submucosa: experimental study. Pediatr Surg Int. 2006; 22(7):593–9. [PubMed: 16773371]

Caissie R, Gingras M, Champigny MF, Berthod F. In vivo enhancement of sensory perception recovery in a tissue-engineered skin enriched with laminin. Biomaterials. 2006; 27(15):2988–93. [PubMed: 16448695]

Carlson BM. Some principles of regeneration in mammalian systems. Anat Rec B New Anat. 2005; 287(1):4–13. [PubMed: 16308859]

Carmeliet P. Blood vessels and nerves: common signals, pathways and diseases. Nat Rev Genet. 2003; 4(9):710–20. [PubMed: 12951572]

Chunzheng G, Shengzhong M, Yinglian J, Ji EW, Jianmin L. Siatic nerve regeneration in rats stimulated by fibrin glue containing nerve growth factor: An experimental study. Injury. 2008

Clarke KM, Lantz GC, Salisbury SK, Badylak SF, Hiles MC, Voytik SL. Intestine submucosa and polypropylene mesh for abdominal wall repair in dogs. J Surg Res. 1996; 60(1):107–14. [PubMed: 8592400]

Dietz FR. Effect of denervation on limb growth. J Orthop Res. 1989; 7(2):292–303. [PubMed: 2783965]

Donzelli R, Maiuri F, Piscopo GA, de Notaris M, Colella A, Divitiis E. Role of extracellular matrix components in facial nerve regeneration: an experimental study. Neurol Res. 2006; 28(8):794–801. [PubMed: 17288733]

Freytes DO, Badylak SF, Webster TJ, Geddes LA, Rundell AE. Biaxial strength of multilaminated extracellular matrix scaffolds. Biomaterials. 2004; 25(12):2353–61. [PubMed: 14741600]

Garavito ZV, Sutachan JJ, Muneton VC, Hurtado H. Is S-100 protein a suitable marker for adult Schwann cells? In Vitro Cell Dev Biol Anim. 2000; 36(5):281–3. [PubMed: 10937828]

Gilbert TW, Sacks MS, Grashow JS, Woo SL, Badylak SF, Chancellor MB. Fiber kinematics of small intestinal submucosa under biaxial and uniaxial stretch. J Biomech Eng. 2006; 128(6):890–8. [PubMed: 17154691]

Gilbert TW, Stewart-Akers AM, Badylak SF. A quantitative method for evaluating the degradation of biologic scaffold materials. Biomaterials. 2007; 28(2):147–50. [PubMed: 16949150]

Gilbert TW, Stewart-Akers AM, Simmons-Byrd A, Badylak SF. Degradation and remodeling of small intestinal submucosa in canine Achilles tendon repair. J Bone Joint Surg Am. 2007; 89(3):621–30. [PubMed: 17332112]

Gilbert TW, Stewart-Akers AM, Sydeski J, Nguyen TD, Badylak SF, Woo SL. Gene expression by fibroblasts seeded on small intestinal submucosa and subjected to cyclic stretching. Tissue Eng. 2007; 13(6):1313–23. [PubMed: 17518717]

Gomez N, Lu Y, Chen S, Schmidt CE. Immobilized nerve growth factor and microtopography have distinct effects on polarization versus axon elongation in hippocampal cells in culture. Biomaterials. 2007; 28(2):271–84. [PubMed: 16919328]

Goslin K, Schreyer DJ, Skene JH, Banker G. Changes in the distribution of GAP-43 during the development of neuronal polarity. J Neurosci. 1990; 10(2):588–602. [PubMed: 2137532]

Grinnell AD. Dynamics of nerve-muscle interaction in developing and mature neuromuscular junctions. Physiol Rev. 1995; 75(4):789–834. [PubMed: 7480163]

Hadlock TA, Sundback CA, Hunter DA, Vacanti JP, Cheney ML. A new artificial nerve graft containing rolled Schwann cell monolayers. Microsurgery. 2001; 21(3):96–101. [PubMed: 11372069]

Hoffman PN. Expression of GAP-43, a rapidly transported growth-associated protein, and class II beta tubulin, a slowly transported cytoskeletal protein, are coordinated in regenerating neurons. J Neurosci. 1989; 9(3):893–7. [PubMed: 2494308]

Jessen KR, Mirsky R. Schwann cell precursors and their development. Glia. 1991; 4(2):185–94. [PubMed: 1851727]

Johansson F, Carlberg P, Danielsen N, Montelius L, Kanje M. Axonal outgrowth on nano-imprinted patterns. Biomaterials. 2006; 27(8):1251–8. [PubMed: 16143385]

Kingham PJ, Terenghi G. Bioengineered nerve regeneration and muscle reinnervation. J Anat. 2006; 209(4):511–26. [PubMed: 17005023]

Kochupura PV, Azeloglu EU, Kelly DJ, Doronin SV, Badylak SF, Krukenkamp IB, Cohen IS, Gaudette GR. Tissue-engineered myocardial patch derived from extracellular matrix provides regional mechanical function. Circulation. 2005; 112(9 Suppl):I144–9. [PubMed: 16159807]

Kropp BP, Eppley BL, Prevel CD, Rippy MK, Harruff RC, Badylak SF, Adams MC, Rink RC, Keating MA. Experimental assessment of small intestinal submucosa as a bladder wall substitute. Urology. 1995; 46(3):396–400. [PubMed: 7660517]

Kropp BP, Rippy MK, Badylak SF, Adams MC, Keating MA, Rink RC, Thor KB. Regenerative urinary bladder augmentation using small intestinal submucosa: urodynamic and histopathologic assessment in long-term canine bladder augmentations. J Urol. 1996; 155(6):2098–104. [PubMed: 8618344]

La Fleur M, Underwood JL, Rappolee DA, Werb Z. Basement membrane and repair of injury to peripheral nerve: defining a potential role for macrophages, matrix metalloproteinases, and tissue inhibitor of metalloproteinases-1. J Exp Med. 1996; 184(6):2311–26. [PubMed: 8976186]

Lantz GC, Badylak SF, Coffey AC, Geddes LA, Blevins WE. Small intestinal submucosa as a small-diameter arterial graft in the dog. J Invest Surg. 1990; 3(3):217–27. [PubMed: 2078544]

Lantz GC, Badylak SF, Coffey AC, Geddes LA, Sandusky GE. Small intestinal submucosa as a superior vena cava graft in the dog. J Surg Res. 1992; 53(2):175–81. [PubMed: 1405606]

Li F, Li W, Johnson S, Ingram D, Yoder M, Badylak S. Low-molecular-weight peptides derived from extracellular matrix as chemoattractants for primary endothelial cells. Endothelium. 2004; 11(3–4):199–206. [PubMed: 15370297]

Lopes MF, Cabrita A, Ilharco J, Pessa P, Paiva-Carvalho J, Pires A, Patricio J. Esophageal replacement in rat using porcine intestinal submucosa as a patch or a tube-shaped graft. Dis Esophagus. 2006; 19(4):254–9. [PubMed: 16866856]

McCaig CD. Myoblasts and myoblast-conditioned medium attract the earliest spinal neurites from frog embryos. J Physiol. 1986; 375:39–54. [PubMed: 3795063]

Mukouyama YS, Shin D, Britsch S, Taniguchi M, Anderson DJ. Sensory nerves determine the pattern of arterial differentiation and blood vessel branching in the skin. Cell. 2002; 109(6):693–705. [PubMed: 12086669]

Navarro X, Vivo M, Valero-Cabre A. Neural plasticity after peripheral nerve injury and regeneration. Prog Neurobiol. 2007; 82(4):163–201. [PubMed: 17643733]

Ota T, Gilbert TW, Badylak SF, Schwartzman D, Zenati MA. Electromechanical characterization of a tissue-engineered myocardial patch derived from extracellular matrix. J Thorac Cardiovasc Surg. 2007; 133(4):979–85. [PubMed: 17382638]

Patrick CW, Zheng B, Schmidt M, Herman PS, Chauvin BP, Fan Z, Stark B, Evans GR. Dermal fibroblasts genetically engineered to release nerve growth factor. Ann Plast Surg. 2001; 47(6):660–5. [PubMed: 11756838]

Phillips JB, Bunting SC, Hall SM, Brown RA. Neural tissue engineering: a self-organizing collagen guidance conduit. Tissue Eng. 2005; 11(9–10):1611–7. [PubMed: 16259614]

Ponomareva ON, Fischer TM, Lai C, Rimer M. Schwann cell-derived neuregulin-2alpha can function as a cell-attached activator of muscle acetylcholine receptor expression. Glia. 2006; 54(6):630–7. [PubMed: 16944454]

Pope, JCt; Davis, MM.; Smith, ER., Jr; Walsh, MJ.; Ellison, PK.; Rink, RC.; Kropp, BP. The ontogeny of canine small intestinal submucosa regenerated bladder. J Urol. 1997; 158(3 Pt 2):1105–10. [PubMed: 9258151]

Prevel CD, Eppley BL, Summerlin DJ, Jackson JR, McCarty M, Badylak SF. Small intestinal submucosa: utilization for repair of rodent abdominal wall defects. Ann Plast Surg. 1995; 35(4):374–80. [PubMed: 8585680]

Recknor JB, Sakaguchi DS, Mallapragada SK. Directed growth and selective differentiation of neural progenitor cells on micropatterned polymer substrates. Biomaterials. 2006; 27(22):4098–108. [PubMed: 16616776]

Record RD, Hillegonds D, Simmons C, Tullius R, Rickey FA, Elmore D, Badylak SF. In vivo degradation of 14C-labeled small intestinal submucosa (SIS) when used for urinary bladder repair. Biomaterials. 2001; 22(19):2653–9. [PubMed: 11519785]

Reddy LV, Koirala S, Sugiura Y, Herrera AA, Ko CP. Glial cells maintain synaptic structure and function and promote development of the neuromuscular junction in vivo. Neuron. 2003; 40(3):563–80. [PubMed: 14642280]

Reing JE, Zhang L, Myers-Irvin J, Cordero KE, Freytes DO, Heber-Katz E, Bedelbaeva K, McIntosh D, Dewilde A, Braunhut SJ, Badylak SF. Degradation Products of Extracellular Matrix Affect Cell Migration and Proliferation. Tissue Eng Part A. 2008 Epub Jul 24.

Robinson KA, Li J, Mathison M, Redkar A, Cui J, Chronos NA, Matheny RG, Badylak SF. Extracellular matrix scaffold for cardiac repair. Circulation. 2005; 112(9 Suppl):I135–43. [PubMed: 16159805]

Sanes JR. Roles of extracellular matrix in neural development. Annu Rev Physiol. 1983; 45:581–600. [PubMed: 6342525]

Sanes JR. Extracellular matrix molecules that influence neural development. Annu Rev Neurosci. 1989; 12:491–516. [PubMed: 2648958]

Schnell E, Klinkhammer K, Balzer S, Brook G, Klee D, Dalton P, Mey J. Guidance of glial cell migration and axonal growth on electrospun nanofibers of poly-epsilon-caprolactone and a collagen/poly-epsilon-caprolactone blend. Biomaterials. 2007; 28(19):3012–25. [PubMed: 17408736]

Sellaro TL, Ravindra AK, Stolz DB, Badylak SF. Maintenance of Hepatic Sinusoidal Endothelial Cell Phenotype In Vitro Using Organ-Specific Extracellular Matrix Scaffolds. Tissue Eng. 2007; 13(9): 2301–10. [PubMed: 17561801]

Skene JH, Willard M. Axonally transported proteins associated with axon growth in rabbit central and peripheral nervous systems. J Cell Biol. 1981; 89(1):96–103. [PubMed: 6164683]

Smith RM, Wiedl C, Chubb P, Greene CH. Role of small intestine submucosa (SIS) as a nerve conduit: preliminary report. J Invest Surg. 2004; 17(6):339–44. [PubMed: 15764502]

Son YJ, Trachtenberg JT, Thompson WJ. Schwann cells induce and guide sprouting and reinnervation of neuromuscular junctions. Trends Neurosci. 1996; 19(7):280–5. [PubMed: 8799973]

Sorensen A, Alekseeva T, Katechia K, Robertson M, Riehle MO, Barnett SC. Long-term neurite orientation on astrocyte monolayers aligned by microtopography. Biomaterials. 2007; 28(36): 5498–508. [PubMed: 17905429]

Stupack DG, Cheresh DA. ECM remodeling regulates angiogenesis: endothelial integrins look for new ligands. Sci STKE 2002. 2002; (119):PE7.

Su Y, Zeng BF, Zhang CQ, Zhang KG, Xie XT. Study of biocompatibility of small intestinal submucosa (SIS) with Schwann cells in vitro. Brain Res. 2007; 1145:41–7. [PubMed: 17367764]

Suzuki M, Satoh A, Ide H, Tamura K. Nerve-dependent and -independent events in blastema formation during Xenopus froglet limb regeneration. Dev Biol. 2005; 286(1):361–75. [PubMed: 16154125]

Triolo D, Dina G, Lorenzetti I, Malaguti M, Morana P, Del Carro U, Comi G, Messing A, Quattrini A, Previtali SC. Loss of glial fibrillary acidic protein (GFAP) impairs Schwann cell proliferation and delays nerve regeneration after damage. J Cell Sci. 2006; 119(Pt 19):3981–93. [PubMed: 16988027]

Ueno T, de la Fuente SG, Abdel-Wahab OI, Takahashi T, Gottfried M, Harris MB, Tatewaki M, Uemura K, Lawson DC, Mantyh CR, Pappas TN. Functional evaluation of the grafted wall with porcine-derived small intestinal submucosa (SIS) to a stomach defect in rats. Surgery. 2007; 142(3):376–83. [PubMed: 17723890]

Valentin JE, Badylak JS, McCabe GP, Badylak SF. Extracellular matrix bioscaffolds for orthopaedic applications. A comparative histologic study. J Bone Joint Surg Am. 2006; 88(12):2673–86. [PubMed: 17142418]

Zantop T, Gilbert TW, Yoder MC, Badylak SF. Extracellular matrix scaffolds are repopulated by bone marrow-derived cells in a mouse model of achilles tendon reconstruction. J Orthop Res. 2006; 24(6):1299–309. [PubMed: 16649228]

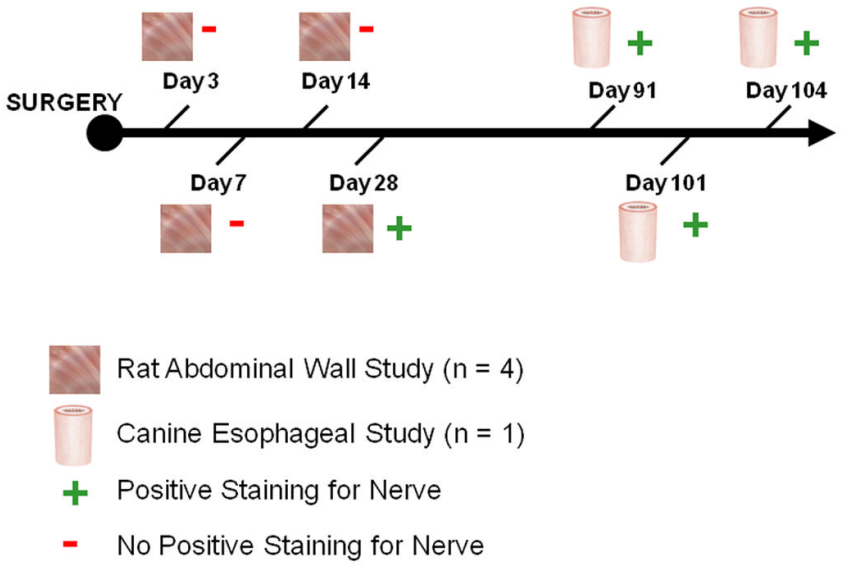

Figure 1.
Timeline for evaluation of innervation in the rat abdominal wall model and the canine esophageal model.

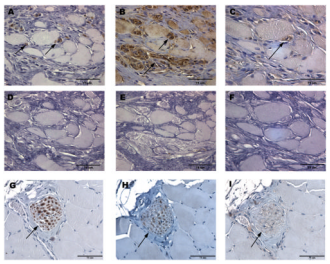

Figure 2.
Histologic images of remodeled UBM 28 days after repair of a 1 cm × 1 cm defect in the rat abdominal wall with specific staining for (A) neurofilament, (B) GAP43, and (C) GFAP. Specificity of staining was confirmed by primary delete negative controls for (D) neurofilament, (E) GAP43, and (F) GFAP. Positive control staining was confirmed in native rat abdominal wall muscle for (G) neurofilament, (H) GAP43, and (I) GFAP. All scale bars are 75 μm.

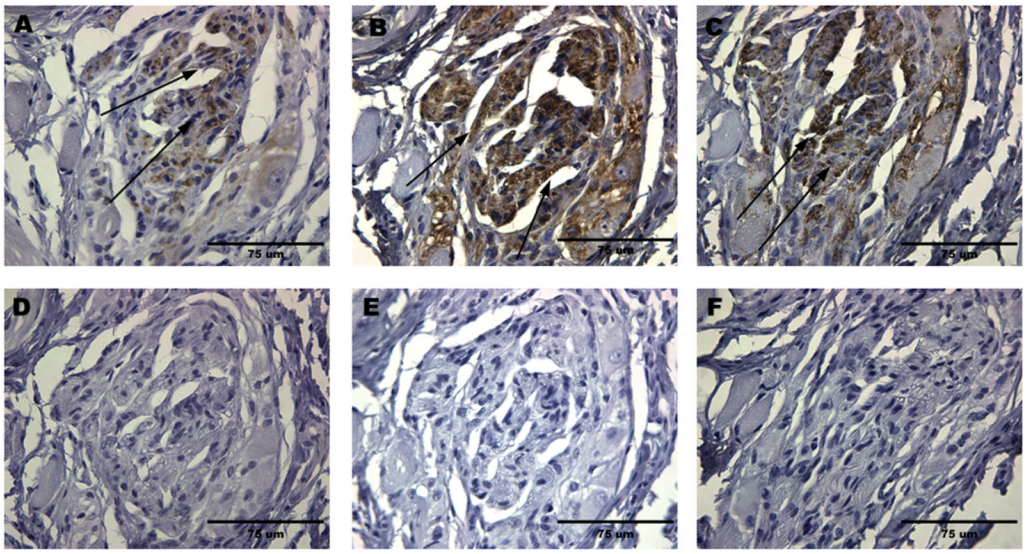

Figure 3.
Histologic images of remodeled UBM 91 days after repair of a 5 cm long canine esophageal endomucosal resection of with removal of 70% of the muscularis externa. Specific staining is shown for (A) neurofilament, (B) GAP43, and (C) GFAP. Specificity of staining was confirmed by primary delete negative controls for (D) neurofilament, (E) GAP43, and (F) GFAP. All scale bars are 75 μm.

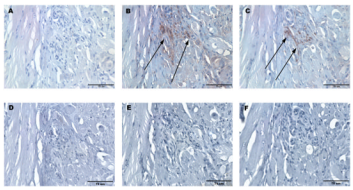

Figure 4.
Histologic images of remodeled UBM 104 days after repair of a 5 cm long canine esophageal endomucosal resection of with removal of 70% of the muscularis externa. Specific staining is shown for (A) neurofilament, (B) GAP43, and (C) GFAP. Specificity of staining was confirmed by primary delete negative controls for (D) neurofilament, (E) GAP43, and (F) GFAP.

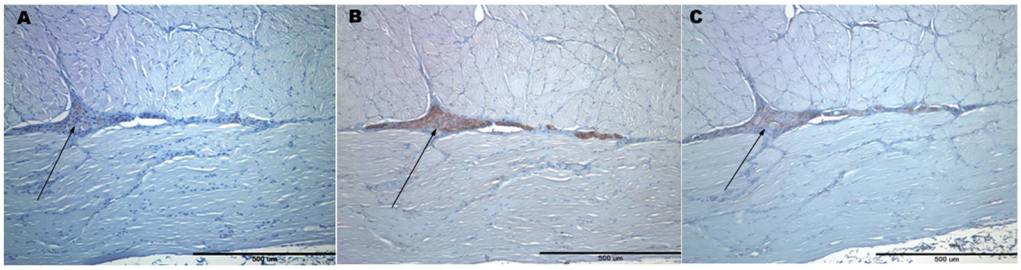

Figure 5.
Histologic images of native esophagus displaying the intramuscular plexus of nerves, with specific staining for (A) neurofilament, (B) GAP43, and (C) GFAP.

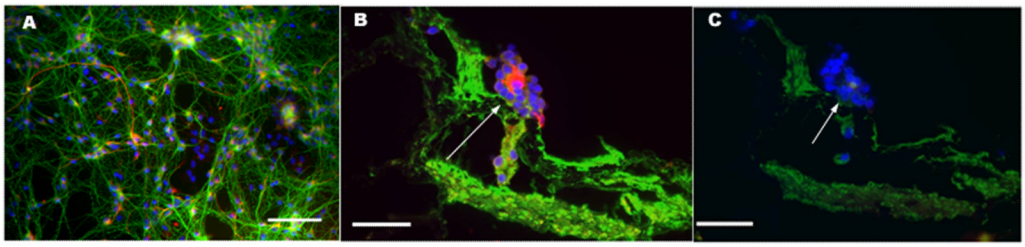

Figure 6.
β-tubulin III (green), glial fibrillary acidic protein (GFAP) (red) and DAPI (blue). (A) Immunofluorescent staining of cells seeded on poly-L-lysine control cover slips after 5 days in culture. (B) Immunofluorescent images of cells seeded on the abluminal surface of the UBM-ECM scaffolds. (C) Immunofluorescent images of seeded sections stained with secondary antibodies only. All scale bars are 50 μm.

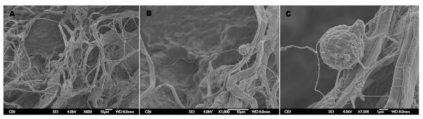

Figure 7.
Scanning electron micrographs of primary spinal cord neurons seeded on the abluminal surface of the UBM scaffold (A–C).

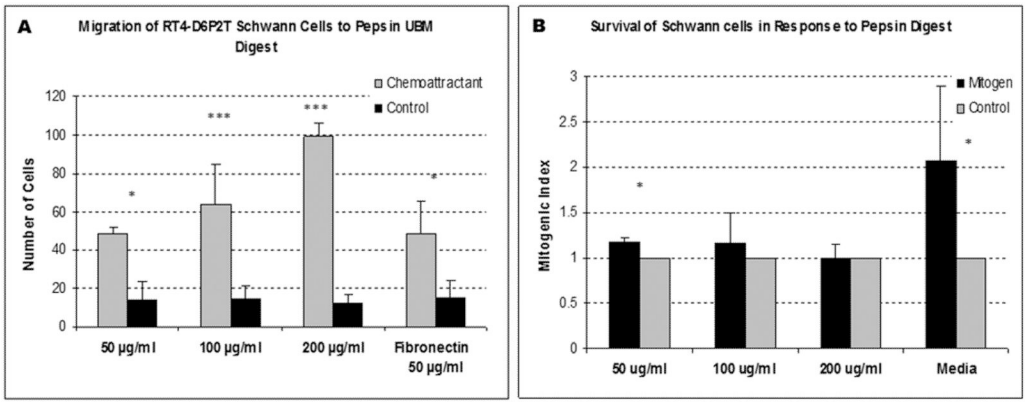

Figure 8.

(A) Migration of Schwann cells towards matricryptic peptides resulting from rapid degradation of UBM or corresponding control. (B) Survival of Schwann cells in the presence of matricryptic peptides resulting from rapid degradation of UBM or corresponding control. (* $p < 0.05$ compared to control, *** $p < 0.005$ compared to control).

Table 1

Surgical groups for canine esophagus and rat abdominal wall studies (Badylak et al., 2005; Brown et al., In press).

Group Number	Surgical Procedure
1	Segmental resection of full thickness canine esophagus, replacement with ECM
2	Segmental removal of full circumference canine endomucosa, muscularis externa left intact, no ECM scaffold
	Segmental removal of full circumference canine endomucosa plus 70% of muscularis externa. ECM scaffold used to replace endomucosa.
3	
4	Segmental removal of full circumference canine endomucosa. ECM scaffold used to replace endomucosa.
5	Partial thickness resection of rat abdominal wall, ECM scaffold used to replace external and internal oblique muscle.